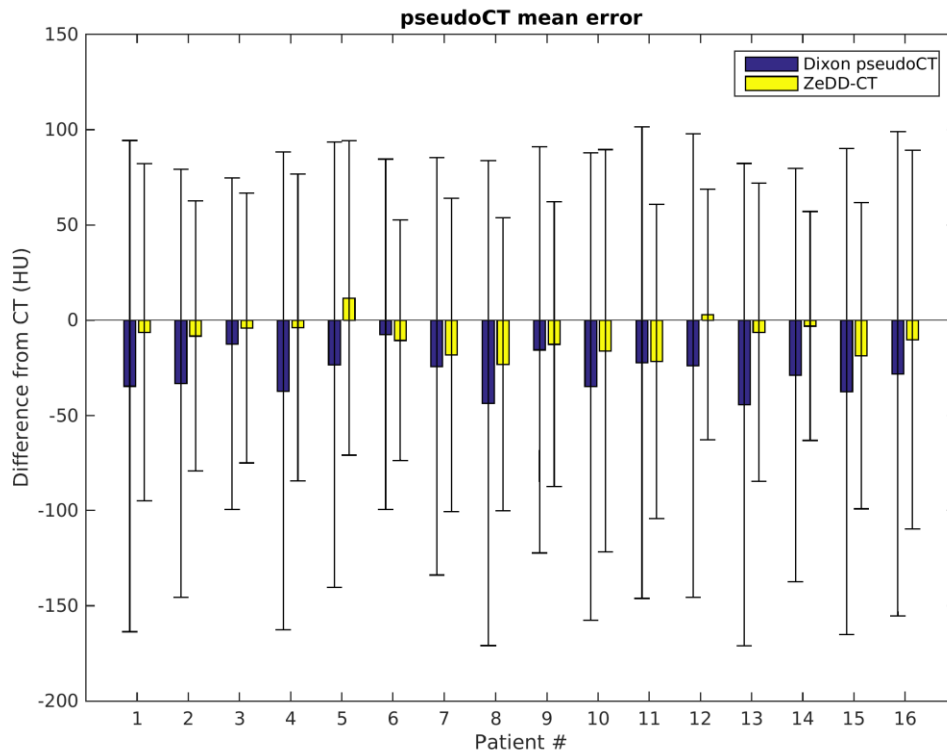
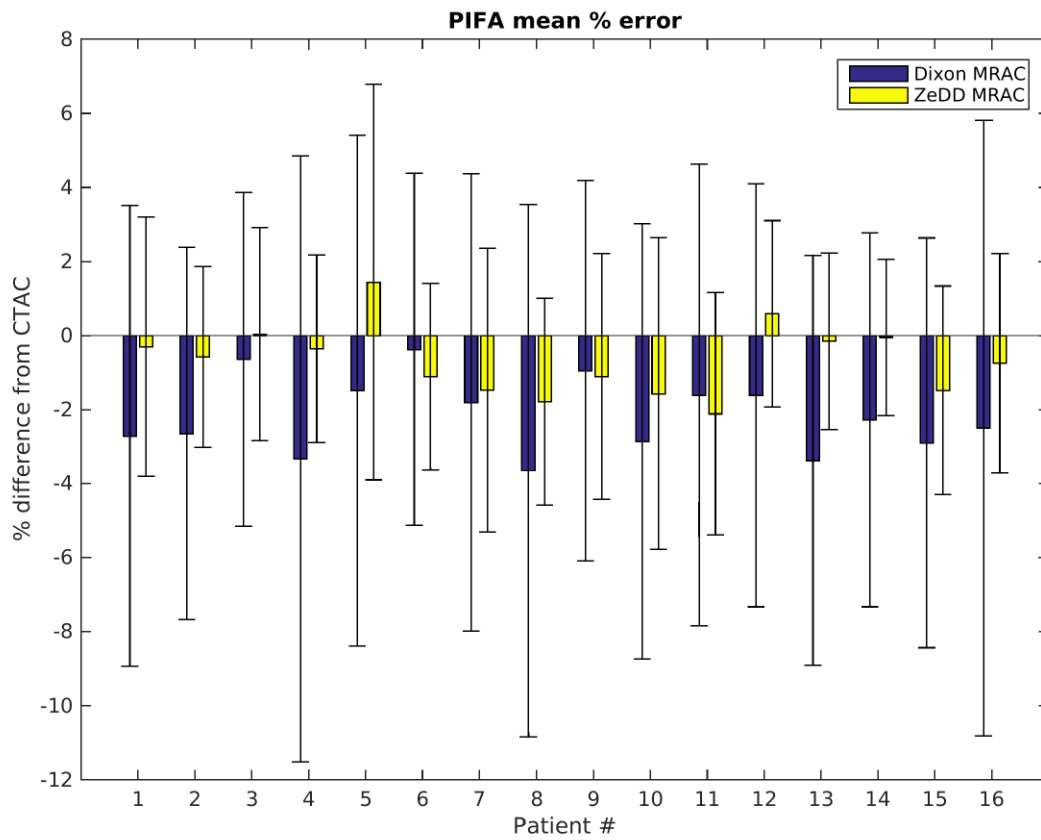


Supplemental Figure 1. PseudoCT mean error for each patient. For each patient, the Dixon pseudoCT is consistently underestimating the Hounsfield units value. The underestimation is reduced in the ZeDD-CT images. The error bars indicate the standard deviation of Hounsfield units. The ZeDD-CT has lower standard deviation than the Dixon pseudoCT.

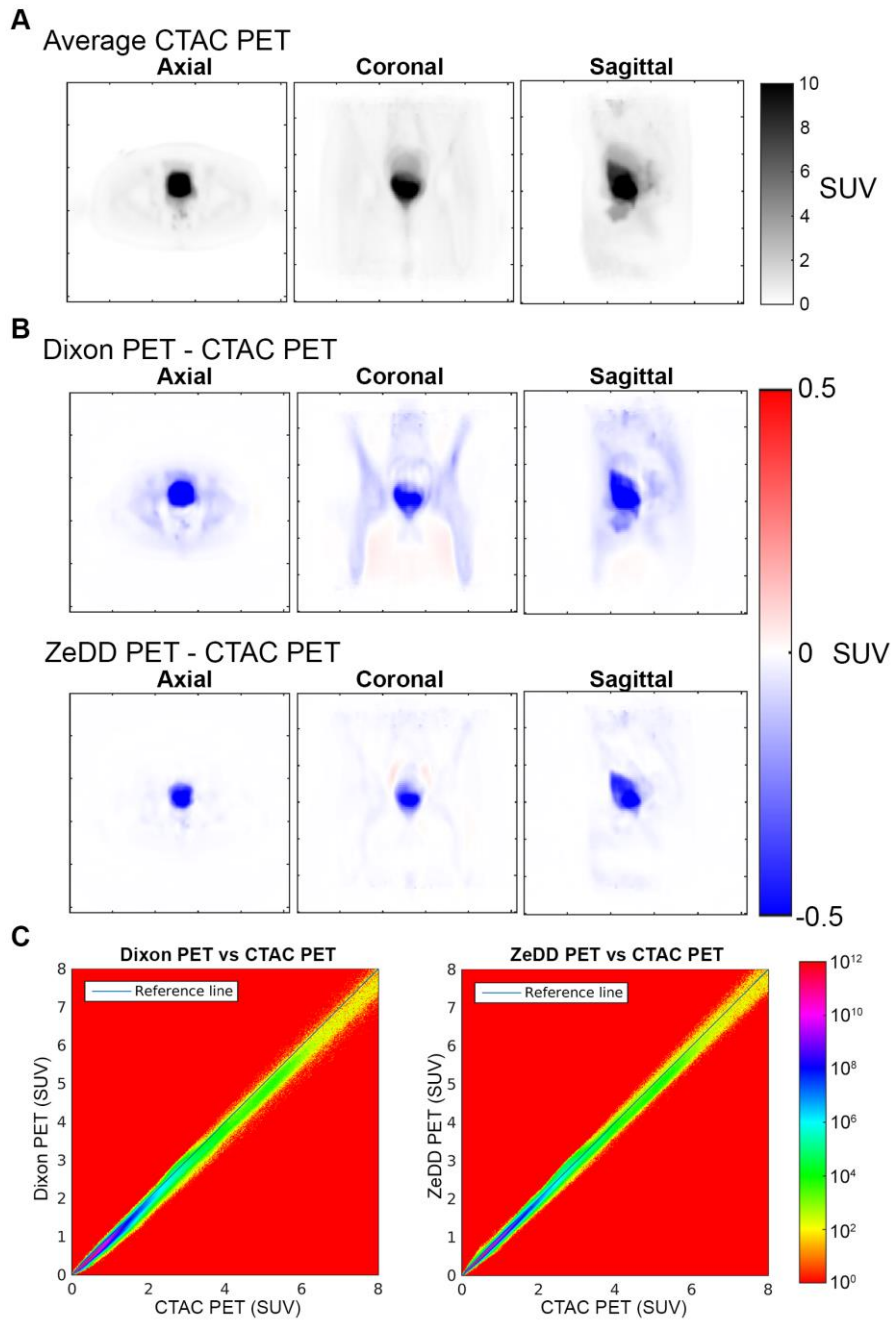


Supplemental Figure 2. Attenuation correction map whole-volume error for each patient.

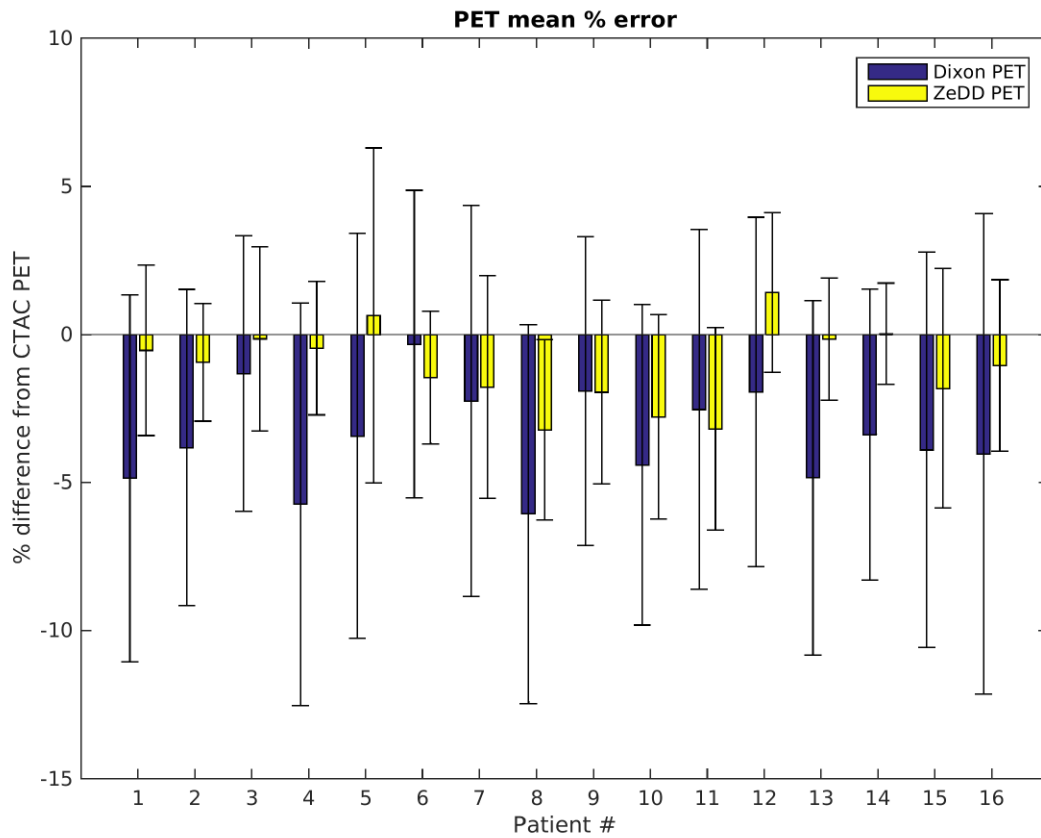
For each patient, the Dixon MRAC is consistently underestimating the Hounsfield units value. The underestimation is reduced in the ZeDD MRAC. The error bars indicate the standard deviation of Hounsfield units. The ZeDD MRAC has lower standard deviation than the Dixon MRAC.



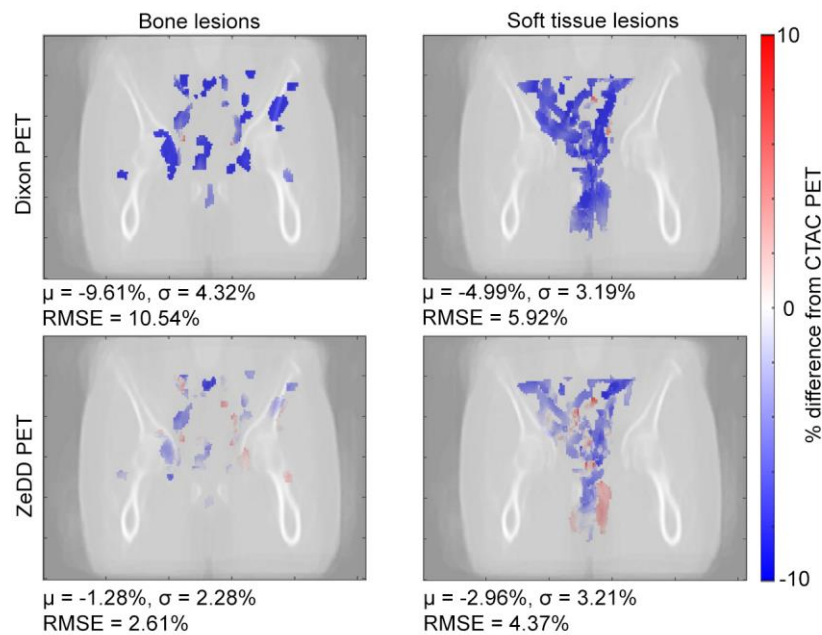
Supplemental Figure 3. Average CTAC PET images from all patients registered to atlas-space (A) and average difference images (B) and joint histograms (C) of Dixon PET and ZeDD PET with CTAC PET. The joint histograms in log-scale (C) show correlation of PET SUV across the whole volume from all patients.



Supplemental Figure 4. PET whole-volume error for each patient. The Dixon PET is consistently underestimating the Hounsfield units value. The underestimation is reduced in the ZeDD PET images. The error bars indicate the standard deviation of Hounsfield units. The ZeDD PET has lower standard deviation than the Dixon PET.

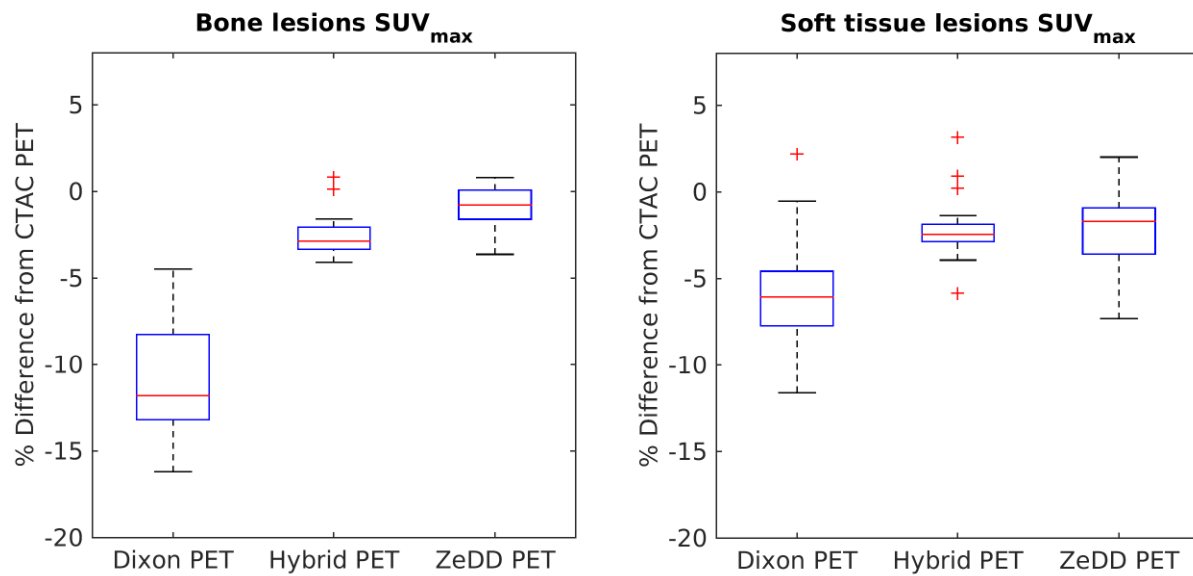


Supplemental Figure 5. Maximum error projections of the lesion error maps for each lesion projected onto the coronal plane are shown. A transparent CT image is overlaid for anatomic reference. The mean bias (μ), standard deviation (σ), and root-mean-squared-error (RMSE) of the uptake in the voxels of each lesion compared to ground-truth are shown below each image. Throughout the whole volume, as with the whole-volume error maps, the lesion uptake was underestimated in the Dixon-based PET.



Supplemental Figure 6. Comparative analysis with Hybrid ZTE/Dixon on lesion SUV_{max} .

In the subset population of 6 patients, 17 bone lesions and 20 soft tissue lesions were identified. ZeDD produces similar results with Hybrid ZTE/Dixon; both methods demonstrate improvement in SUV_{max} uptake estimation over Dixon and is statistically significant.



Supplementary Table 1. Patient demographics, disease diagnoses, and PET radiotracers of the test set.

Patient #	Age	Gender	Disease	Radiotracer
1	56	Male	Lung cancer with bone metastases	¹⁸ F-FDG
2	59	Female	Colon cancer	¹⁸ F-FDG
3	60	Male	Colon cancer	¹⁸ F-FDG
4	56	Male	Rectal cancer	¹⁸ F-FDG
5	58	Male	Rectal cancer	¹⁸ F-FDG
6	58	Female	Rectal cancer	¹⁸ F-FDG
7	54	Female	Rectal cancer	¹⁸ F-FDG
8	69	Male	Prostate cancer	⁶⁸ Ga-PSMA-11
9	70	Male	Prostate cancer	⁶⁸ Ga-PSMA-11
10	60	Female	Cervical cancer	¹⁸ F-FDG
11	83	Male	Prostate cancer	⁶⁸ Ga-PSMA-11
12	62	Male	Prostate cancer	⁶⁸ Ga-PSMA-11
13	51	Female	Ovarian cancer	¹⁸ F-FDG
14	62	Male	Rectal Cancer	¹⁸ F-FDG
15	78	Male	Prostate cancer	⁶⁸ Ga-PSMA-11
16	53	Male	Prostate cancer	⁶⁸ Ga-PSMA-11